GA–A22639

ENERGY BALANCE, RADIATION AND STABILITY DURING RAPID PLASMA TERMINATION VIA IMPURITY PELLET INJECTIONS ON DIII–D

by
D.G. WHYTE, T.E. EVANS, A.G. KELLMAN, D.A. HUMPHREYS,
A.W. HYATT, T.C. JERNIGAN, R.L. LEE, S.L. LUCKHARDT,
P.B. PARKS, M.J. SCHAFFER, and P.L. TAYLOR

JUNE 1997

DISCLAIMER

ENERGY BALANCE, RADIATION AND STABILITY DURING RAPID PLASMA TERMINATION VIA IMPURITY PELLET INJECTIONS ON DIII–D

by
D.G. WHYTE,[†] T.E. EVANS, A.G. KELLMAN, D.A. HUMPHREYS,
A.W. HYATT, T.C. JERNIGAN,[‡] R.L. LEE, S.L. LUCKHARDT,[†]
P.B. PARKS, M.J. SCHAFFER, and P.L. TAYLOR

[†]University of California, San Diego
[‡]Oak Ridge National Laboratory

ENERGY BALANCE, RADIATION AND STABILITY DURING RAPID PLASMA TERMINATION VIA IMPURITY PELLET INJECTIONS ON DIII–D*

D.G. Whyte,[a] T.E. Evans, A.G. Kellman, D.A. Humphreys, A.W. Hyatt, T.C. Jernigan,[b]
R.L. Lee, S.L. Luckhardt,[a] P.B. Parks, M.J. Schaffer, and P.L.Taylor
General Atomics, P.O. Box 85608, San Diego, CA 92138-5608
[a]*University of California, San Diego, California.*
[b]*Oak Ridge National Laboratory, Oak Ridge, Tennessee.*

Injections of impurity "killer" pellets on DIII–D have demonstrated partial mitigation of undesirable disruption phenomena; namely reducing the convected heat loss to the wall, and the halo current's magnitude and toroidal asymmetry. However, the appearance of a runaway electron population and large magnetic fluctuations ($\tilde{B}/B_T \approx 1\%$) is coincident with the measured rapid loss of the plasma's thermal energy ($\approx$1 MJ in 1 ms) due to impurity radiation. A numerical code is developed to simulate the impurity radiation and predict the rapid plasma cooling observed. The simulation predicts two mechanisms for the generation of runaway electrons: the "slideaway" of hot tail electrons due to rapid cooling or the transport of hot electrons into the thermally collapsed plasma due to instabilities. Pressure gradients caused by the rapid non-adiabatic cooling of the impurity are identified as the probable source of these instabilities which also lead to convective heat losses. Results of a modeling effort to optimize pellet content, impurity species and cooling time for the avoidance of instabilities and runaway electrons are shown.

1.   Description of Experiment and Model

Solid impurity pellets of neon and argon are injected at the outer midplane of DIII–D (R = 1.7 m, a = 0.6 m) in an attempt to radiatively quench the plasma. Pellets have diameters of 1.8 mm or 2.7 mm, injection velocity $\approx$500 m/s and typically penetrate to a minor radius r of $0.2 < r/a < 0.5$. Impurity radiation is measured by a calibrated SPRED XUV survey spectrometer which provides 1 ms time resolution over the wavelength range of 100–1100 Å and has a single tangential line of sight with a tangent radius near the magnetic axis (R_{tan} = 1.8 m). Experiments have shown that the use of impurity pellets during Vertical Displacement Events (VDE) [1] reduces the convected thermal loads (measured by infrared thermography) to the divertor by up to a factor of two by increasing the fraction of initial stored energy which is radiated by the impurity. The induced poloidal halo current's magnitude and toroidal asymmetry are also reduced. Pellet injection into steady-state plasmas (i.e. pre-emptive) also show large fractions (50%–80%) of the energy radiated. However, experimental indications of runaway electron production (i.e. hard X-ray bursts, non-thermal ECE emissions) are greatly increased, especially in the case of preemptive pellet injections.

A time dependent model (Killer Pellet RADiation, KPRAD) is used to simulate the radiation and energy balance during pellet injection experiments on a given flux surface (no radial

transport). The calculation first solves the ionization charge-state equilibrium for the impurity species and the subsequent radiative losses from each charge state (i.e. coronal equilibrium is not assumed). Then a new self-consistent energy balance including radiation losses, ohmic heating and collisional coupling between all species is calculated at each timestep. The new plasma solution for density and temperature is then used for the subsequent timestep's ionization balance. The code independently considers as separate species the original electrons and ions, as well as the impurity ions and the electrons contributed from their ionization. The amount of deposited pellet atoms on the flux surface is determined by using the standard pellet ablation model [2] normalized to obtain the measured penetration radius. Radiation rates for each charge state k, L_k (Wm^3) are extracted from the ADPAK [3]] atomic database. The electron density, n_e, and each charge state's density n_k are used to calculate the radiated power $P_{rad,k} = n_k\,n_e\,L_k$ (Wm^{-3}). Initial plasma parameters (n_{e0}, T_{e0}, j_0) are taken from measurements and the local current density, j, is held proportional to the measured total plasma current I_p, (i.e. $j(t) = j_0 \cdot I_p(t)/I_{p0}$). Ohmic heating power ($P_{ohmic}$) and the parallel electric field (E) are derived from Spitzer resistivity ($\eta \propto Z_{eff} T_e^{-3/2}$, $P_{ohmic} = \eta j^2$, $E = \eta j$) using the calculated electron temperature and Z_{eff}. The code predicts the time evolutions of electron and ion temperature, electron density, average charge state of impurity, total radiation, and radiation per charge state.

2. Results

The focus of this section will be the comparison of modeling results and experimental data for a preemptive radiative quench following the injection of a small (1.8 mm diam., $N_{pellet} \approx 2 \times 10^{20}$, $N_{plasma} \approx 10^{21}$, v = 390 m/s) neon pellet which penetrated to r/a $\approx$ 0.45. Figure 1 shows the model predicts the measured rapid decrease of the core temperature and plasma energy in ≤0.5 ms. The reason for this thermal collapse is that the high radiation rate of the low ionization stages of neon ($L_{0-7} \approx 10^{-31}\,Wm^3$) and the large amount of pellet material deposited decrease the electron temperature quickly enough to inhibit ionization into or past the He-like state (two electrons), where the radiation efficiency is much lower

Fig. 1. Calculated T_e and average ion charge state Z_i at r/a = 0.6 vs. time after pre-emptive neon pellet passes that flux surface. Square indicates Thomson measured T_e at r/a = 0.6 and the bar the range in core T_e showing complete thermal collapse in core.

($L_{8-10} \approx 10^{-33}\,Wm^3$). This is confirmed experimentally by the absence of any line radiation from these high charge states. The background ion temperature (T_i) and the electrons contributed from neon ionization $T_{e,Neon}$ are quickly thermalized to the main electrons through collisions and the total thermal energy of the plasma is lost to radiation. After the thermal collapse a new equilibrium is established between radiated power and the enhanced
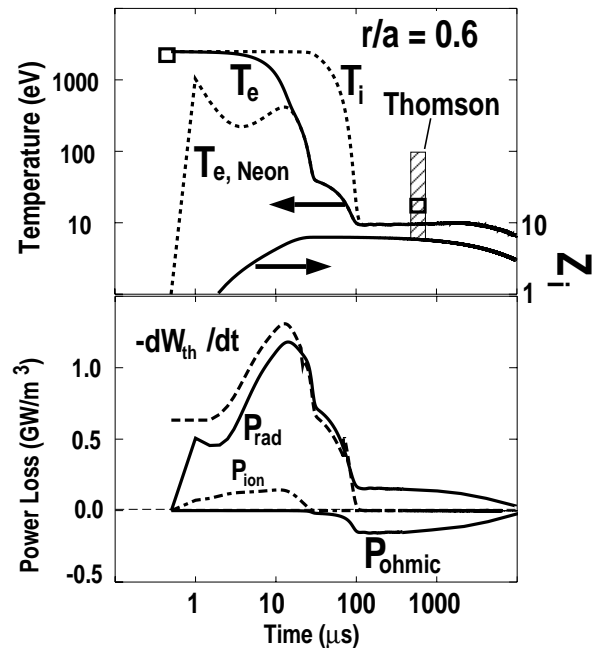
ohmic heating (from the now highly resistive plasma) and no further significant temperature decrease is expected. A comparison of the measured and calculated radiation (Fig. 2) shows good agreement in the magnitude and time behavior of the total and charge specific radiation. This indicates that indeed a large portion of the initial thermal energy is lost to radiation. Also, the significant amount of radiation well into the current quench shows that plasma magnetic energy is also being depleted via radiation. Finally, the relative increase in the radiation of the lower charge states during the current quench indicates volume recombination taking place in a very cold and dense core plasma.

The rapid thermal collapse of the plasma will cause large pressure gradients to form during the pellet ablation (Fig. 3) and drive associated instabilities (e.g. ballooning modes, etc.). The magnitude of this pressure gradient will be determined by the cooling rate of the pellet material, $\tau_{cooling}$ ($\Delta P/\Delta r \approx P_O/\Delta r \propto P_O/\tau_{cooling}$) with typical $\Delta r \approx 0.1$ m $\ll a$. This is verified experimentally (Fig. 4) by the increasing measured magnitude of n=1 modes during preemptive ablation for larger pellets and pellets made of argon ($L_{Ar} \approx 3 \cdot L_{Ne}$).

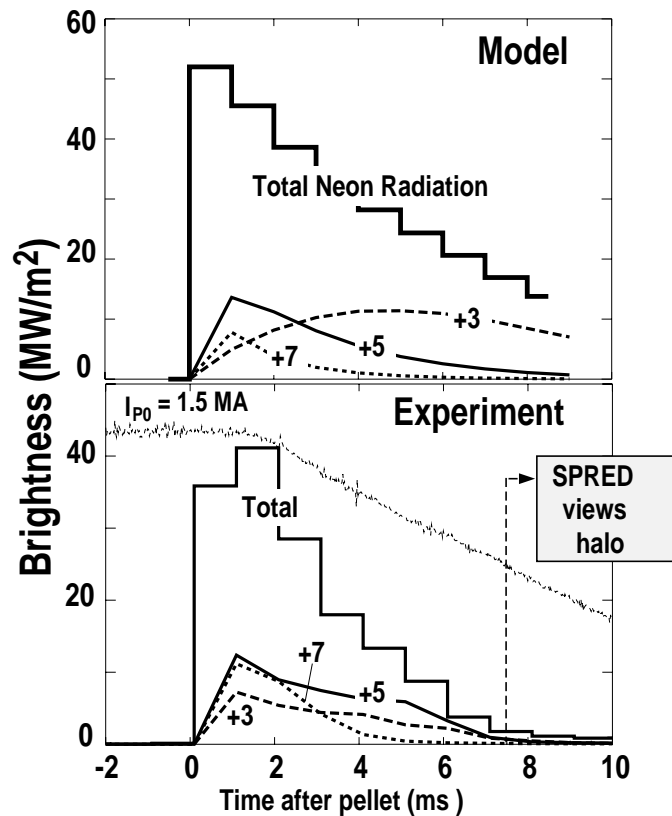The increased production of runaway electrons is also linked to the

Fig. 2. Comparison of neon radiation between experiment and modeling. Experimental brightnesses of charge states are relative from resonance transitions. At t =7 ms the core plasma has moved out of SPRED's view.
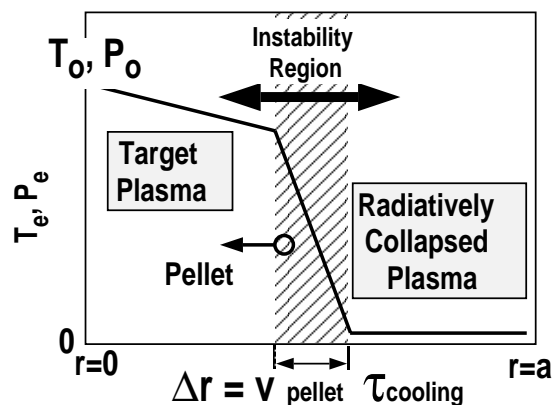

Fig. 3 Schematic of pellet moving through plasma. Rapidly cooled plasma behind pellet causes pressure gradients and instabilities.

cooling rate (Fig. 4). This can stem from two phenomena. Figure 5 shows that a portion of the original Maxwellian tail ($>12\cdot T_e$) electrons will have too weak collisional coupling to the bulk electrons and can cross over the runaway critical energy ε_{crit} which is decreasing due to the enhanced resistivity and electric field. In addition, particle transport caused by large instabilities could place $T_e > \varepsilon_{crit}$ electrons from the hot target plasma into the thermally
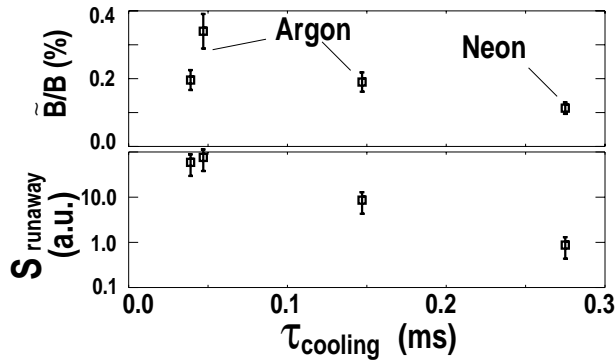
Fig. 4 Measured instability magnitude and runaway source rate increase with faster calculated cooling times. $S_{runaway}$ is obtained from time integrated non-thermal ECE emission during thermal quench.
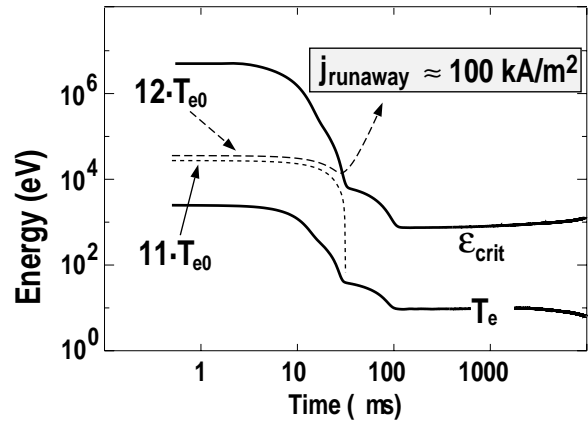

Fig. 5 Test particle calculation shows that rapid cooling can cause portion of original energetic electrons to become suprathermal and carry significant current.

collapsed plasma and also produce runaways. Both of these methods are sensitive to the cooling rate and hence agree with experimental observations.

4.   Discussion

The model shows that pellet cooling is sufficient to thermally collapse the plasma over the penetration radius while simultaneously producing ∇P instabilities that cause the loss of the remaining thermal energy. A sufficiently rapid radiative loss is needed to quench the plasma, but the associated large pressure gradients from excessive cooling during the pellet ablation should be avoided since they lead to enhanced convected losses

Fig. 6 Ratio of final to initial plasma thermal energy (W_f/W_0) and normalized energy loss rate vs. relative amount of deposited pellet material (N_{dep}) to local electrons (N_e).

and runaways. Therefore, the pellet species must be carefully selected in order to optimize the radiative quench, since the cooling rate is primarily determined by the atomic physics of the material. Figure 6 shows the predicted response of a DIII–D plasma (T_e = 2 keV) to various amounts of pellet material and different pellet compositions. In the amount of pellet material deposited (for Ne and Ar experiments: $0.4 \leq N_{dep}/N_e \leq 1$), there exists a small region over which there is sufficient cooling ($W_f/W_0 \leq 0.2$) in a typical thermal quench time $\tau_{TQ} \approx 1$ ms, but also acceptable cooling rates [$dW/dt \cdot (\tau_{TQ}/W_0) \lesssim 1$ are experimentally verified to not cause instabilities]. There does not exist the experimental precision to design the pellet ablation this carefully. Methane pellets however seem to exhibit the desired behavior over a large and achievable range of pellet deposition.
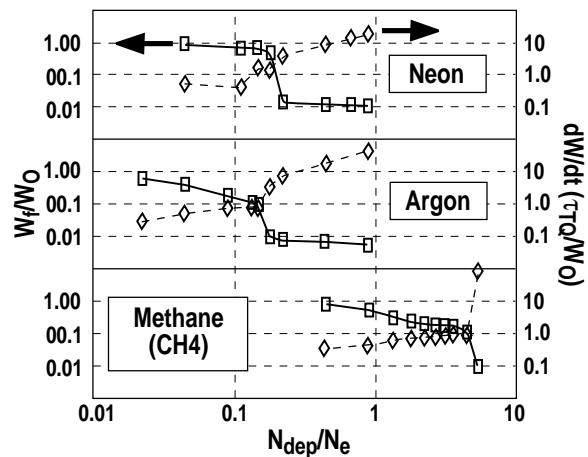
[1]   Kellman, A.G., *et al.* "Disruption Studies in DIII-D," in Proc. of the 16th IAEA Fusion Energy Conf. , Montreal, Canada 1996, to be published.
[2]   Kuteev, B.V., *et al.*, Nucl. Fusion **35** (1995) 1167.
[3]   Hulse, R.A., *et al.*, Nucl. Technology/Fusion **3** (1983) 259.